22p

X63 16853
Code 2A

STATE-OF-THE-ART 1963

STRUCTURES AND MATERIALS

(NASA TMX 50985)

by R. R. Heldenfels*
Chairman, AIAA Technical Committee on Structures

and A. Hurlich**
Member, AIAA Technical Committee on Materials

INTRODUCTION

Significant progress has been made in many areas of structures and materials technology in the past year, but no breakthroughs were evident. Advances in structural analysis and design occurred for all types of flight vehicles with particular emphasis on the problems of supersonic transports, hypersonic aircraft, launch vehicles, reentry vehicles, orbital space stations and lunar excursion vehicles. Materials developments encompassed the invention and commercialization of new metallic alloys, glasses and polymeric materials, and the modification and improvement of existing materials to increase their strength, range of usefulness and fabricability. The multitude of contributions cannot be adequately treated in this short article, consequently, only a few of the important recent developments will be discussed.

The authors wish to acknowledge the contributions of their fellow committee members, who provided much valuable material, to the preparation of this article.

* Chief, Structures Research Division, NASA Langley Research Center, Hampton, Virginia

**Chief of Materials and Structures Research, General Dynamics/Astronautics, San Diego, California

STRUCTURES

Structural Design Criteria and Reliability

The importance of reliability in the design of space systems has led to analytical assessments of the reliability of various structures. The results have shown that, as one might expect, the reliability of structures designed under the time-honored, safety-factor philosophy varies greatly. This variation comes from different degrees of statistical scatter in the loading and strength of various types of structures.

The established structural design criteria for static loading consists of first determining a limit load that is not expected to be exceeded in service and applying a factor of safety to determine the ultimate load. The structure is then designed to avoid failure under the ultimate load and excessive deformation under limit load. This approach involves a certain amount of arbitrariness and may result in either unnecessary weight penalties or low structural reliability.

Figure 1, from work done at the Martin Company, is a plot of structural reliability versus the ratio between the standard deviation and mean value of the failing load for a case in which the applied load is non-statistical and the "allowable" load is assumed to be the 99% value. A design with a factor of safety of one would have a reliability, therefore, of 0.99. With a factor of safety of 1.25 (typical of missile construction) the reliability is strongly dependent on the relative width of the scatter band. If a simple tension member of wrought metal is being designed, the value of the abscissa might be about 0.5 and the reliability would be very high (0.999999). If, on the other hand, a thin monocoque cylinder in compression is being designed, the appropriate value might be 0.20 and the reliability is considerably lower (0.999). The use of a uniform factor of safety is clearly inappropriate in a balanced design.

Plots like Figure 1 can also be prepared for cases in which the applied load is also statistical in nature and used to determine the factor of safety needed to obtain the desired reliability. While much progress has been made in the use of statistical techniques to put structural design criteria on a reliability basis, much work remains to be done to include repeated loadings, time dependent effects, fatigue, creep and multivariate loadings in a rational way.

Meteoroid Impact and Penetration

Design criteria to insure the safety of spacecraft subjected to meteoroid bombardment must necessarily be put on a reliability basis. The principal problem in developing such criteria, however, is the determination of the penetrating power of the debris in space. Major progress was made in this direction with Explorer XVI (S-55B) which transmitted data from December 16, 1962 until July 23, 1963. This NASA satellite has provided unique statistical data on the penetration of thin metallic surfaces in orbital flight.

Explorer XVI was launched with 160 small pressurized cylinders for penetration sensors covering 17 square feet of the surface; several other detection systems covered smaller areas. These cylinders were made of beryllium copper with 100 having material 0.001 inch thick, 40 with 0.002 and

20 with 0.005. Penetrations were obtained on 44 of the 1 mil, 11 on the 2 mil, and none of the 5 mil sensors. Comparison of these results with several theories that have been advanced shows that the data lie between the most optimistic and pessimistic estimates, indicating that the meteoroid puncture problem for thin materials is not nearly as severe as many investigations had postulated.

Other advances have been made in the ground simulation and analysis of meteoroid impact. One of the barriers to progress has been the relatively low velocity (less than 10 km/sec) attainable with most particle acceleration devices such as light gas guns. Recently, devices which utilize electrically exploded foils have achieved velocities in the range of 20 km/sec with small disc-shaped particles. Many problems must be solved, particularly in the area of precise definition of particle characteristics such as size, shape and velocity, before these devices will yield definitive data on hypervelocity impact. However, it now appears that the exploding foil gun has the potential to adequately simulate meteoroid impact in a ground facility.

After several years in which little progress was made, many investigators are now working on hypervelocity impact theories and some significant advances have been made. Recent results were reported at the Sixth Hypervelocity Impact Symposium in May 1963 and at the AIAA Summer Meeting in June 1963. Of note is the work of Walsh and Tillotson in which they conclude that the volume of the crater in a semi-infinite target is very nearly proportional to the projectile kinetic energy. This directly contradicts the results reported earlier by Bjork in which the crater volume was proportional to projectile momentum. Future resolution of this disagreement between the two analyses should significantly advance our understanding of the basic processes involved.

Despite much progress, the rational design of spacecraft to resist meteoroid damage is still dependent on the development of considerable technology. Good experimental studies at high velocities (25-50 km/sec) are urgently needed to support the theoretical studies now underway as is more data on meteoroid damage in flight. Knowledge that could be gained from an examination of recovered structures, damaged by meteoroids during space flight, would be a major contribution.

Properties of Composite Structures

The past year has seen an increased effort devoted to structural analysis of composite materials to define the mechanical properties of the composite from the properties of the constituents. Elastic constants have been obtained for uniaxially reinforced fibrous composites and approximate values of the elastic modulus have been derived for composites containing fibers in a three dimensional array that also includes the effects of the matrix.

The experimental approach has been advanced by investigations of residual shrinkage stresses, stress concentrations near broken fibers, modes of failure and the effect of geometry upon stiffness. Also, microscopic observations of fibers during the fracture process has added understanding of composite failure. Figure 2 (from work at General Electric - MSD) shows the random distribution of internal fiber fractures prior to failure of a thin glass reinforced plastic sample. The fiber diameters are large compared to the minimum distance between them. They are viewed by transmitted polarized light where dark regions correspond to low stresses in the vicinity of the fracture. These fractures were initially observed at about half the ultimate load level.

High Temperature Structures

Recent developments in high temperature structures have been characterized by design, fabrication and testing of large structural components. The Martin Company is constructing a multiwall structural component designed by NASA-Langley. This component, to be tested by NASA, contains a tank for liquid hydrogen and has the capability of sustaining temperatures in excess of 2500° F on parts of the outer surface. The Martin Company is also designing and building a fuselage and wing root component for the USAF that will be tested by Aeronautical Systems Division. This component is a hot monocoque structure containing a liquid hydrogen tank. These components are part of the joint USAF-NASA effort to advance the technology of hypersonic air-breathing vehicles.

The high temperature structure for actual flight vehicles have made significant advances also. The hot structure of the X-20 (Dyna-Soar) has been designed and is now being fabricated by Boeing. Fabrication has also been completed on similar structures for the USAF ASSET vehicle, Figures 3 and 4, the first of which is scheduled to be flown before this article is published. In the ASSET program, six small glide vehicles, all having the same external configuration, will be flown in a critical portion of the reentry flight corridor to advance the structures and materials technology of lifting reentry vehicles. The vehicles have been designed, fabricated and instrumented by McDonnell. A wide variety of metallic and non-metallic materials will be used on these vehicles; maximum external surface temperatures ranging from 1000° F on the aft bulkhead to 3700° F at the nose tip will be encountered. Of particular interest are skin panels of coated molybdenum and columbium alloys and the graphite-zirconia nose cap.

Shell Structures

Substantial amounts of analysis and some testing continue to be devoted to shell structures. The widespread interest in this subject is indicated by three recent conferences on the subject. NASA-Langley held a Symposium on the Instability of Shell Structures in October 1962; the 4th Annual structures and materials meeting of the AIAA, April 1963, was a Launch and Space Vehicle Shell Structures Conference, and in August 1963, the Lockheed Missile and Space Company sponsored a Conference on Shell Theory and Analysis.

With continued attack by many investigators, the unsolved problems of shell analysis are slowly yielding. For example, the long standing search for the correct first approximation linear shell theory has apparently ended with general agreement that the theory proposed independently by Sanders and Koiter is the best. Recently, also, the results of more complete analysis have provided new insight into two problems of long standing in shell stability, that is, the analysis of the assymetrical buckling of spherical shells under external pressure by both Weinitschke and Huang and the proper consideration of boundary conditions in the buckling of cylinders under axial compression by both Stein and Fischer.

A fresh viewpoint is also developing on shell buckling experiments with the recognition that much of the data collected in the past has been almost useless in clarifying the problem. Sechler has demonstrated that much can be learned if the experimenter is willing to use sufficient care; for example, his tests on very thin cylinders under axial compression have yielded buckling loads of over 80% of those predicted by classical linear theory.

The newer forms of construction, however, such as sandwich and filament wound shells have not been receiving a sufficient share of the recent work. Particularly needed is good experimental data on these configurations.

MATERIALS

Constructional Metals

Aluminum alloys have long been used for the fuel and oxidizer tankage of non-cryogenic and cryogenic liquid propelled vehicles. These alloys consisted in the main of the non-heat treatable aluminum-magnesium 5000 series alloys and the high strength, heat treatable 2014 aluminum-copper alloy. The former are too low in strength for satisfactory application in aerospace vehicles, while the latter suffers from restricted weldability and weld embrittlement at cryogenic temperatures and under multi-axial stress conditions.

The 2219 aluminum-copper alloy, first used in the Bomarc surface-to-air missile, is now finding wider application in aerospace vehicles. While somewhat lower in strength than the 2014 aluminum alloy, weldments in the 2219 alloy exhibit considerably improved toughness under bi- and tri-axial loading conditions at reduced temperatures. More recently, the development of a wide family of aluminum-magnesium-zinc alloys of the 7000 series (7002, 7006, 7038, and 7039) has significantly increased the number of high strength, weldable aluminum alloys which possess excellent resistance to brittle fracture, high notch toughness, good mechanical properties in heavy sections, and which can be supplied in the form of sheet, plate, extrusions, and forgings. The new 7000 series alloys possess good combinations of strength, ductility, and toughness in both base metal and weld joints at temperatures at least down to −320° F, and are being evaluated for possible use at liquid hydrogen temperature.

While the very high strength aluminum-copper-magnesium-zinc 7001 alloy has been available for some years, the recent development of the -T75 temper has now provided a high strength aluminum alloy as strong as the 7075-T6 (70,000 psi yield strength and 80,000 psi tensile strength) but with considerably higher resistance to stress corrosion. The 7001 aluminum alloy is not recommended for welding, but it should find wide application in hydraulic and pneumatic systems as tubing, fittings, cylinders, housings, brackets, and fasteners.

The most exciting recent development in alloy steels concerns the "maraging" grades of which three basic compositions are emerging; the 18% nickel-cobalt-molybdenum-titanium, with or without small additions of aluminum, zirconium, and boron, the 20% nickel-titanium-aluminum-columbium, and the 25% nickel-titanium-aluminum-columbium types. The "maraging" alloys have very low carbon contents, and the 18% and 20% nickel grades are essentially martensitic at room temperature while the 25% nickel grade is austenitic after annealing. The lower nickel alloys are strengthened by aging them at 900° F to cause precipitation of complex intermetallic compounds. The 25% nickel alloy must be conditioned by heating to 1100–1300° F, air cooling and refrigerating at -100° F to precipitate intermetallic compounds and cause transformation to martensite. Subsequent aging develops high strengths. The "maraging" steels can be heat treated to strengths in the range of 250,000 to 300,000 psi, and can develop even higher strengths by combinations of cold working and aging after annealing. These steels are formable and weldable in the annealed condition and develop up to 95% tensile efficiency in weld joints after aging. They exhibit higher notch toughness than other alloy steels at corresponding strength levels and show very promising ductility and resistance to brittle fracture down to extreme sub-zero temperatures. Burst tests on scale model pressure vessels have demonstrated the extrem[illegible] "maraging" steels, and it is expected that these steels w[illegible] cases and other airborne pr[illegible]

Improvements have been made in a number of titanium alloys such that they are now satisfactory for application down to liquid hydrogen temperature. The development of the ELI (extra low impurity) grades of the 5Al-2.5Sn-titanium and the 6Al-4V-titanium grades, which was sparked by work done at General Dynamics/Astronautics with the cooperation of the titanium industry, has resulted in alloys possessing excellent combinations of strength-to-weight ratio, ductility, and resistance to brittle fracture in both base metal and weld joints down to extreme subzero temperatures.

Recent work at Lockheed Missile and Space Co. on beryllium has led to the development of a Be-Al alloy containing approximately 33% Al (Lockalloy) which has a density of 0.074 lbs/in.^{3}, an elastic modulus of 29×10^6 psi, yield strength of 40,000 psi and tensile strength of 50,000 psi, with 4-8% elongation. Higher strengths with lower ductility are developed by extrusion. This alloy may find use in compression loaded or other structures where stiffness is a requirement.

High temperature metals have also undergone considerable development and improvement. The Inconel 718 nickel base alloy can be strengthened by combinations of cold working and aging to strengths up to approximately 250,000 psi. This alloy exhibits good strength, ductility, and fracture toughness over the temperature range of -423° F to 1300° F, and can be used in applications exposed to service temperatures through this range. Dispersion hardened alloys are also becoming of practical significance with TD nickel, containing a few percent of thoria very finely dispersed in a matrix of nickel, possessing useful engineering properties at temperatures up to within a few hundred degrees of the melting point of nickel. This alloy also is very ductile and notch tough at temperatures down to -423° F. While dispersion hardened alloys lose their elevated temperature strengths in weld joints, considerable progress has been made in joining them by brazing.

Refractory Metals, Protective Coatings, and Ceramics

The manufacture of the X-20 (Dynasoar) glide vehicle is resulting in the development of fabrication experience with two refractory alloys, columbium-10Ti-5Zr (D 36) used in applications heated within the range of approximately 1900°-2700° F and molybdenum-0.5Ti-0.1Zr (TZM) for use in applications between 2700° to 3000° F. In this vehicle, the requirements consist of adequate strength at service temperatures to sustain aerodynamic loads, oxidation resistance, and high emittance to efficiently radiate heat.

Formability and weldability were considered to be of secondary importance, with deficiencies circumvented by appropriate design and manufacture.

The Boeing Co. has developed a fluidized bed method for coating refractory metal parts with silicide type coatings. Figure 5 shows a schematic of the fluidized bed facility and Figure 6 is a photograph of the inside of the reactor. Silicon carbide dispersed in a silicon dioxide sol is sprayed over a simple silicide coating then fused in air at 2000° F. The coated refractory alloys have been successfully tested in an environmental simulator (see Figure 7) which duplicated glide reentry conditions with pressures ranging from 10^{-5} to 750 mm of mercury and temperatures ranging up to 3000° F. Work at Lockheed had demonstrated that many promising oxidation resistant coatings failed under the low pressure high-gas-flow conditions of lift reentry after having performed well under ambient pressure conditions.

A new type of metal-ceramic composite has been developed by Boeing which appears capable of combining strength and fabrication advantages of the cermet and the increased reliability of reinforced ceramic systems. This composite is the "macro-laminate system" wherein alternate layers of powdered metals and ceramic oxides in thin sheets are broken into small particles and compacted by hot pressing techniques into a composite body. A molybdenum-hafnia body thus produced exhibits excellent thermal shock properties, thermal stability to 4000° F for 30 minutes, room temperature compressive deformation of 14.5%, room temperature compressive ultimate of 1.4×10^5 psi, flexural ultimate of 5×10^4 psi at room temperature and 9000 psi at 3000° F.

Glass and Polymeric Materials

A number of significant developments have been made in glass which will lead to important improvements in filament wound aerospace vehicle structures. These include the development of the Owens-Corning S-994 high strength glass which contains 10% MgO and the YM-31A high modulus glass which contains BeO. The former glass is approximately 30% higher in strength than the E-glass which has been widely used in filament wound rocket motor cases, and this higher strength has been realized in full scale 54" diameter pressure vessels fabricated from the S-994 filament. Filament wound epoxy laminated structures made with the S-994 glass have developed strength-to-weight ratios of 2.3×10^6 in.lbs/lb as compared to approximately 1.1×10^6 for high strength steel and titanium alloys.

The development of higher modulus glass is of considerable importance since the large radial expansion of rocket motor cases may crack the propellant and result in excessively rapid combustion or explosion of the motors. Experimental laminates made with the YM-31A glass have demonstrated a 20 to 40% increase in elastic modulus over E-glass laminates.

While it is still high experimental, recent work at Aeronautical Systems Division on boron filaments produced by a vapor deposition process and bonded with epoxy resins showed that very high strength and high modulus values could be achieved. Preliminary calculations show that composite rocket motor cases fabricated from boron and S-994 glass filaments could be significantly lighter in weight yet flexurally stiffer than the strongest titanium alloy case currently made.

In the field of resins, films, and adhesives, the recent advent of the polybenzimidazole and polyoxydiazole polymers has greatly extended their useful temperature range. The Imidite (trade name of Narmco Division of Telecomputing Corp.) adhesives and glass laminates can be used continuously at temperatures up to 700° F and intermittently at temperatures up to 1500° F with useful engineering properties at these temperatures. DuPont is currently marketing high temperature films (DuPont H film), potting compounds (DuPont polymer SP), as well as Pyre-ML, a coated glass fabric for high temperature electrical insulation applications; with all these materials based on the new polymers. These polymers generally require high temperatures (up to 700° F) and high pressures for curing.

FACTORS OF SAFETY AND RELIABILITY

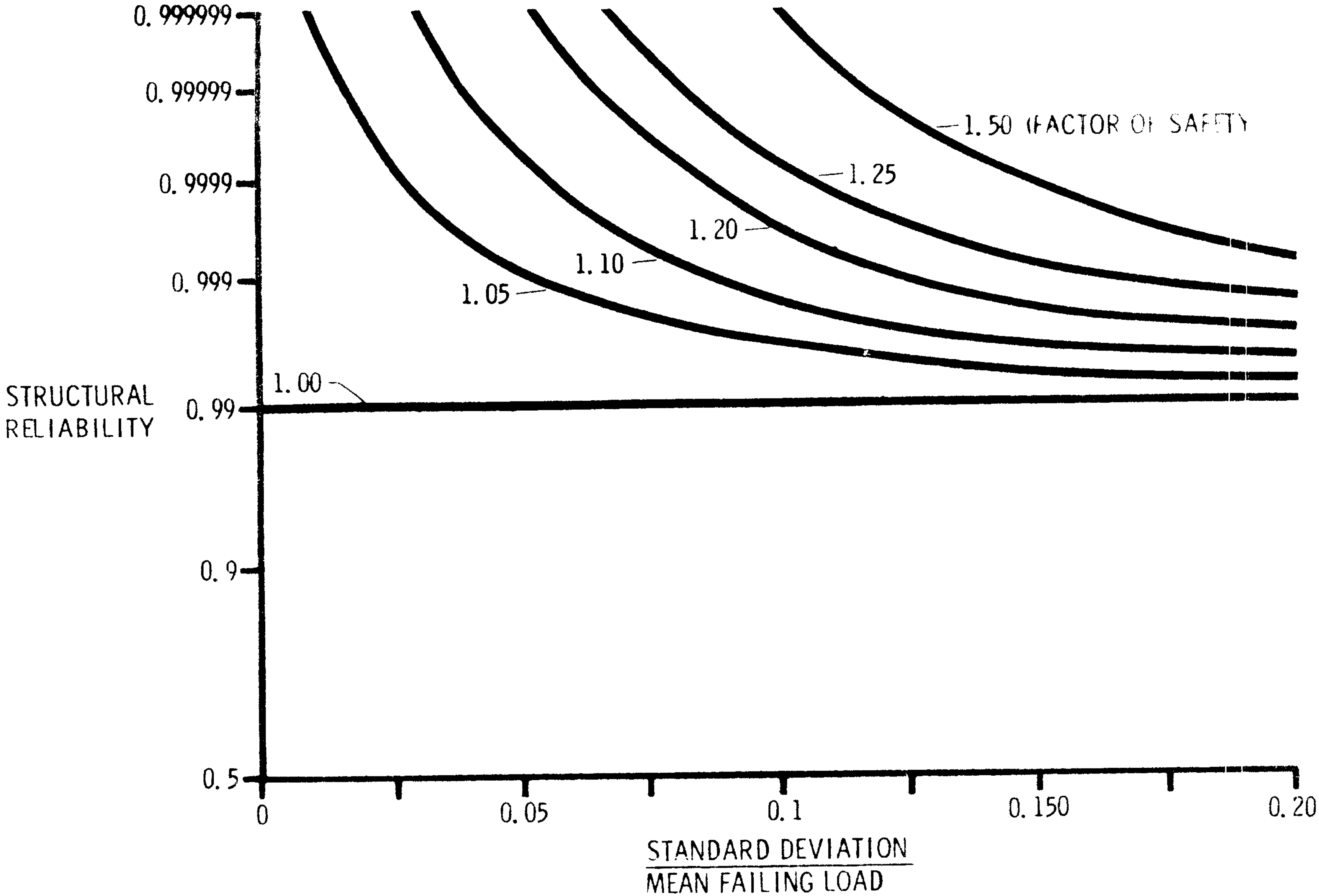

ER 13039

FIG. 1

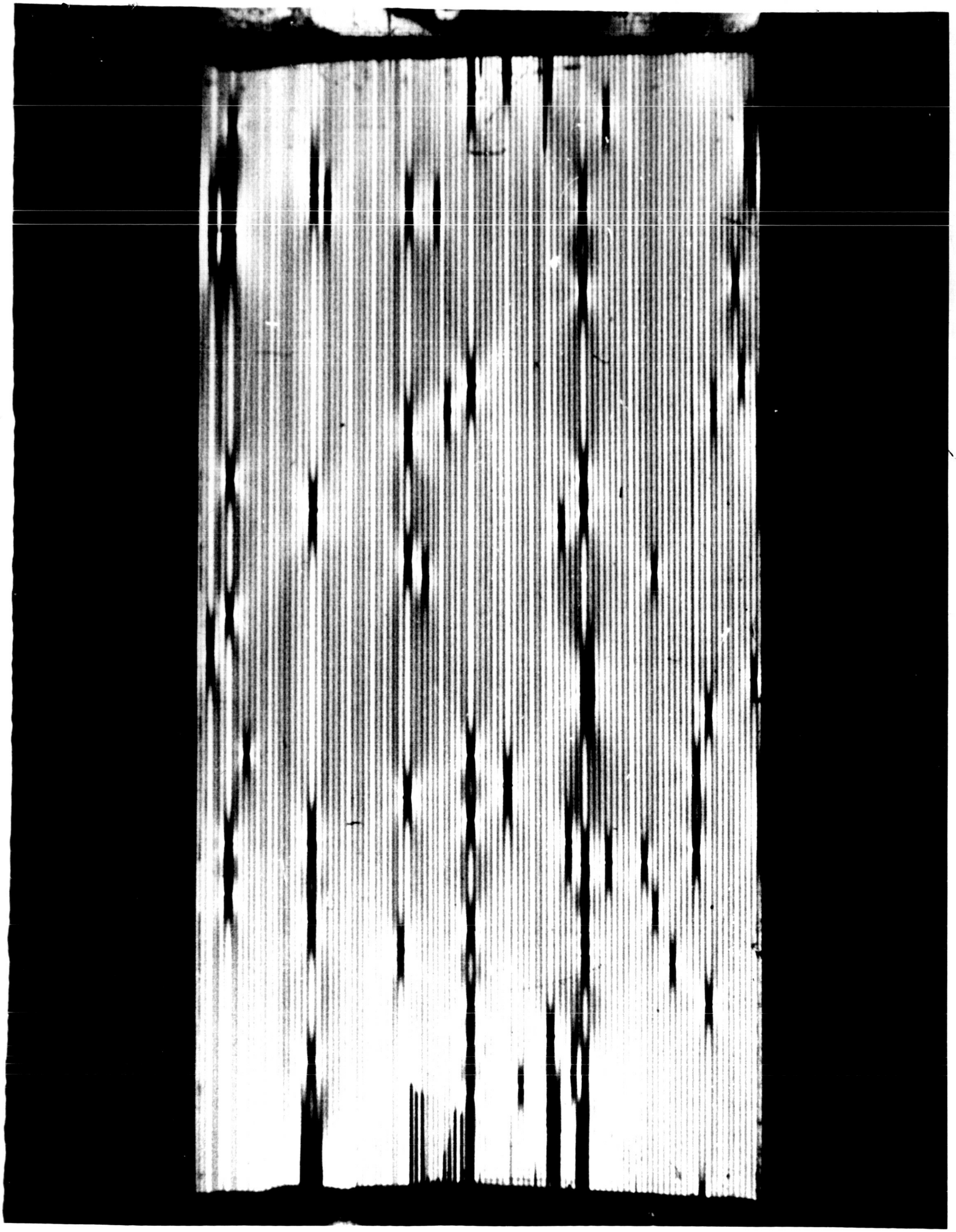

DESIGN CONCEPT

MANUFACTURING BREAKDOWN

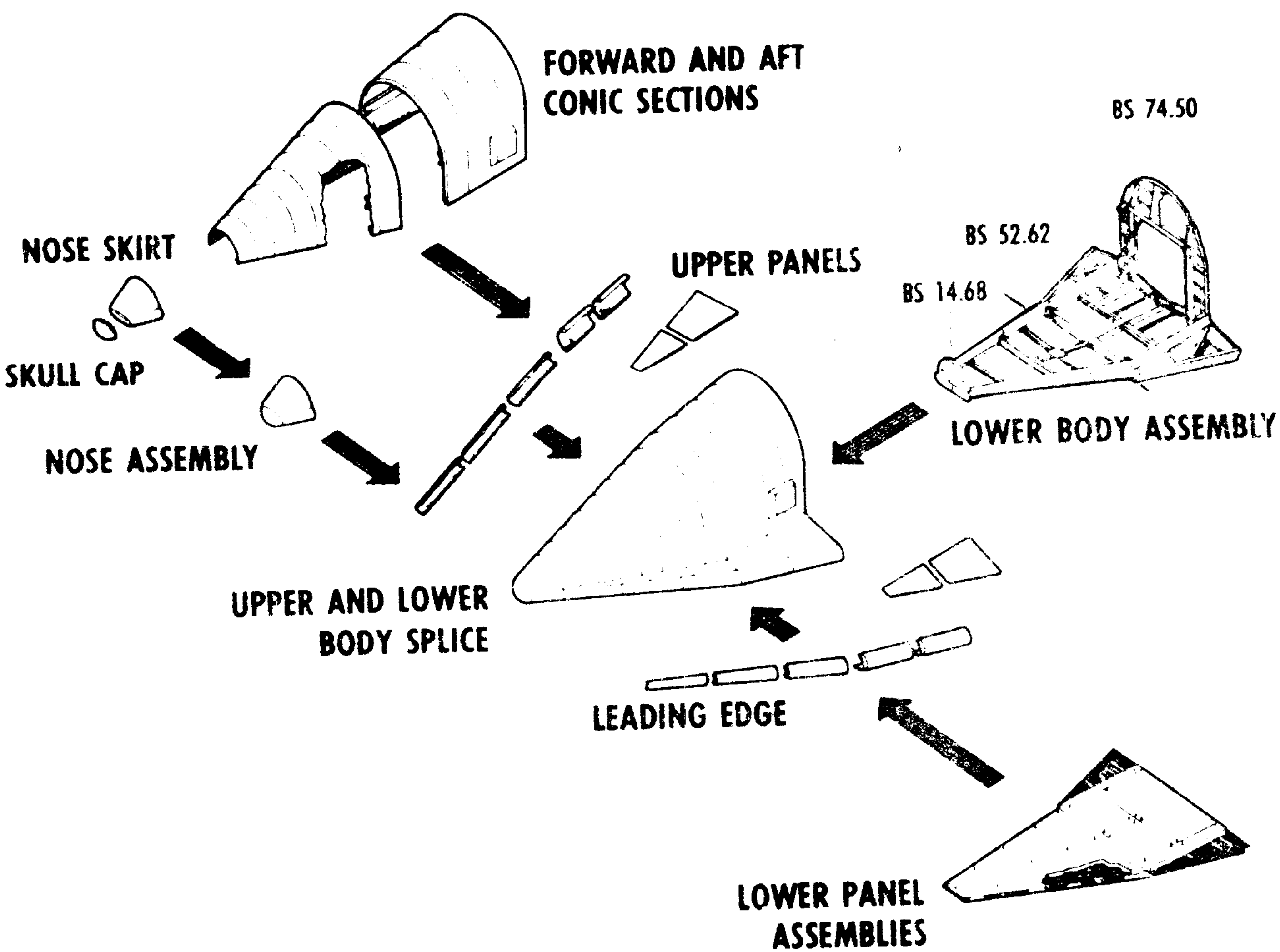

FIG. 3

DESIGN CONCEPT

STRUCTURAL CROSS SECTION

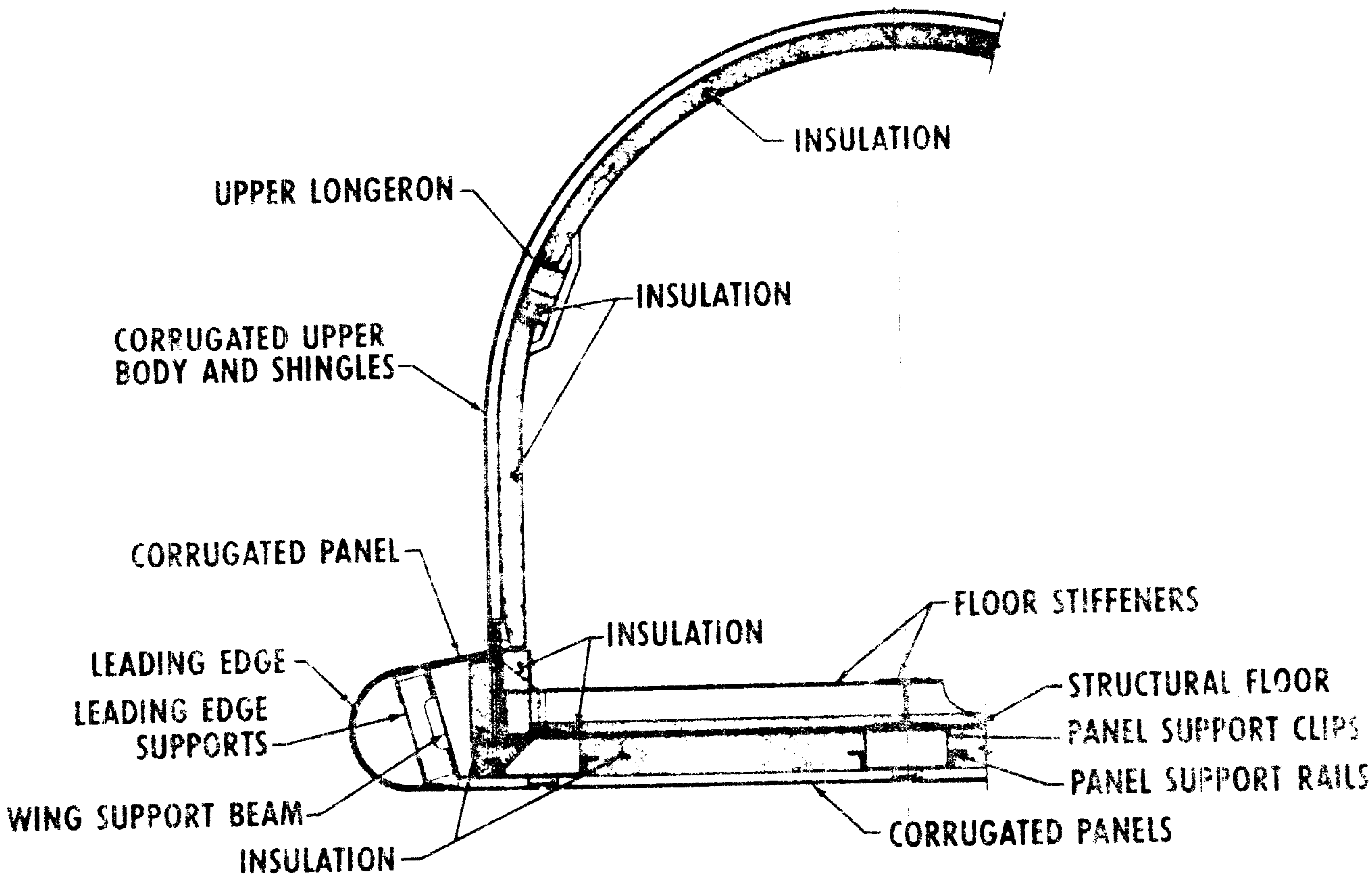

FIG. 4

FIGURE 3 FLUIDIZED BED

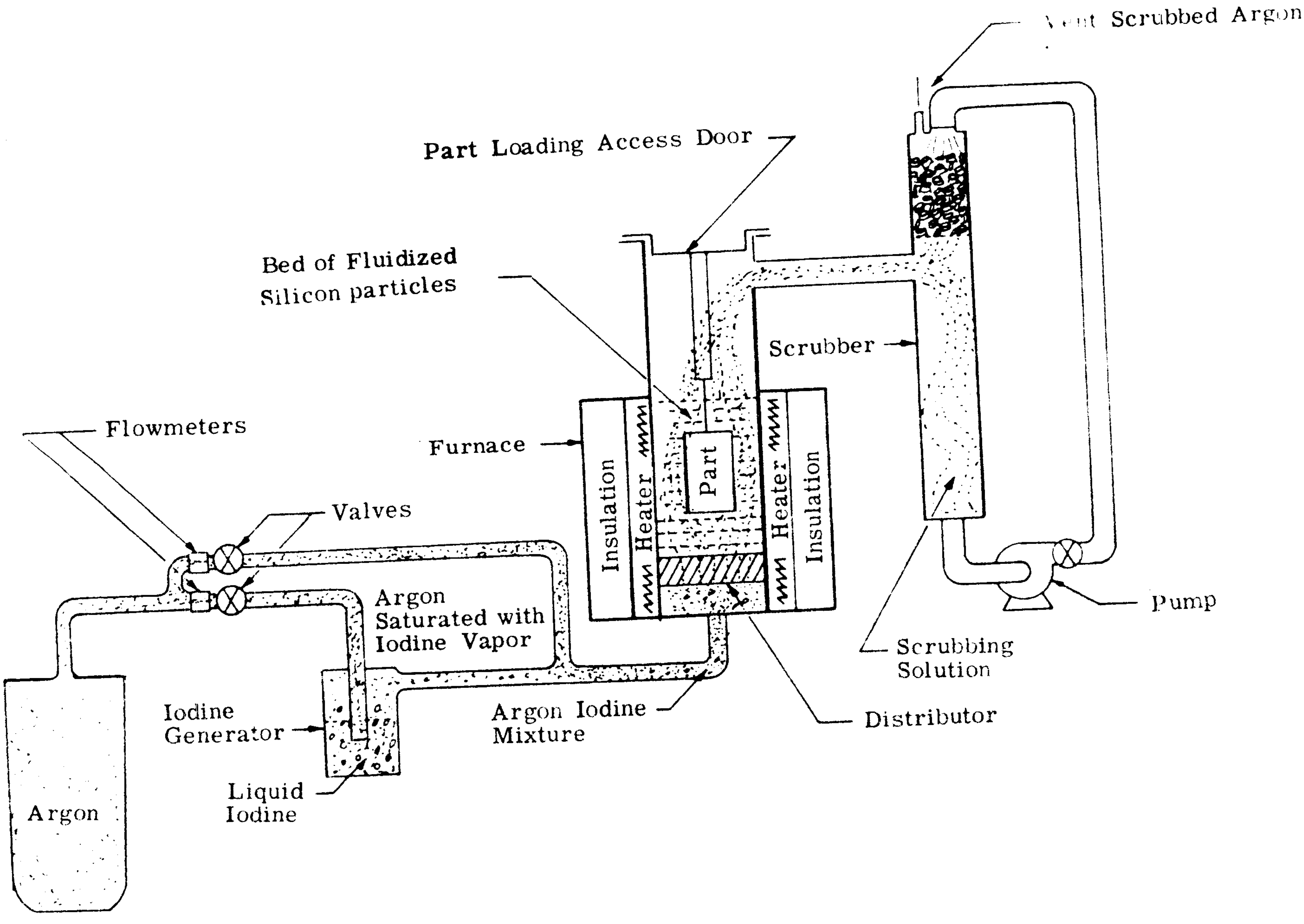

F/G. 5

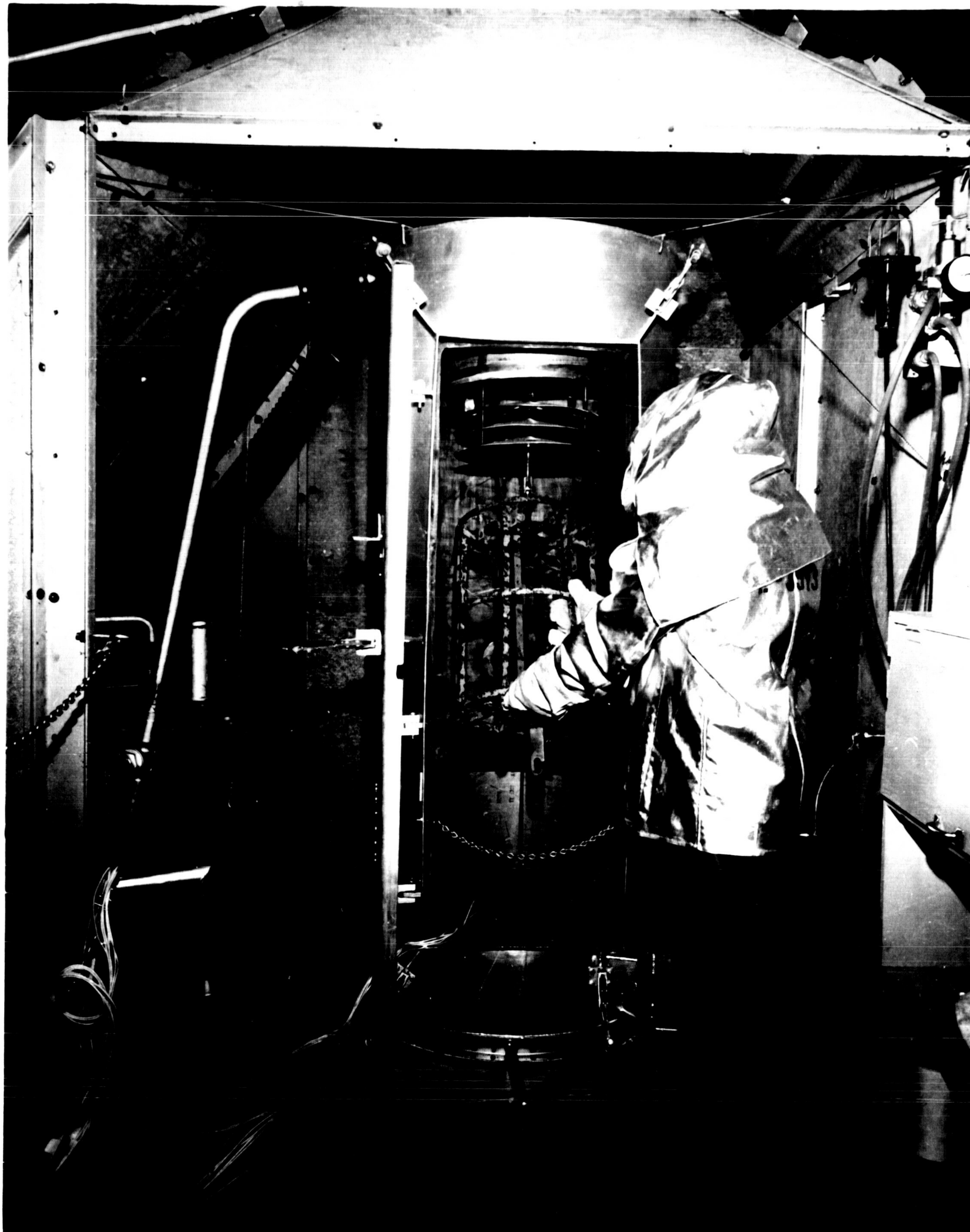

FIG. 6

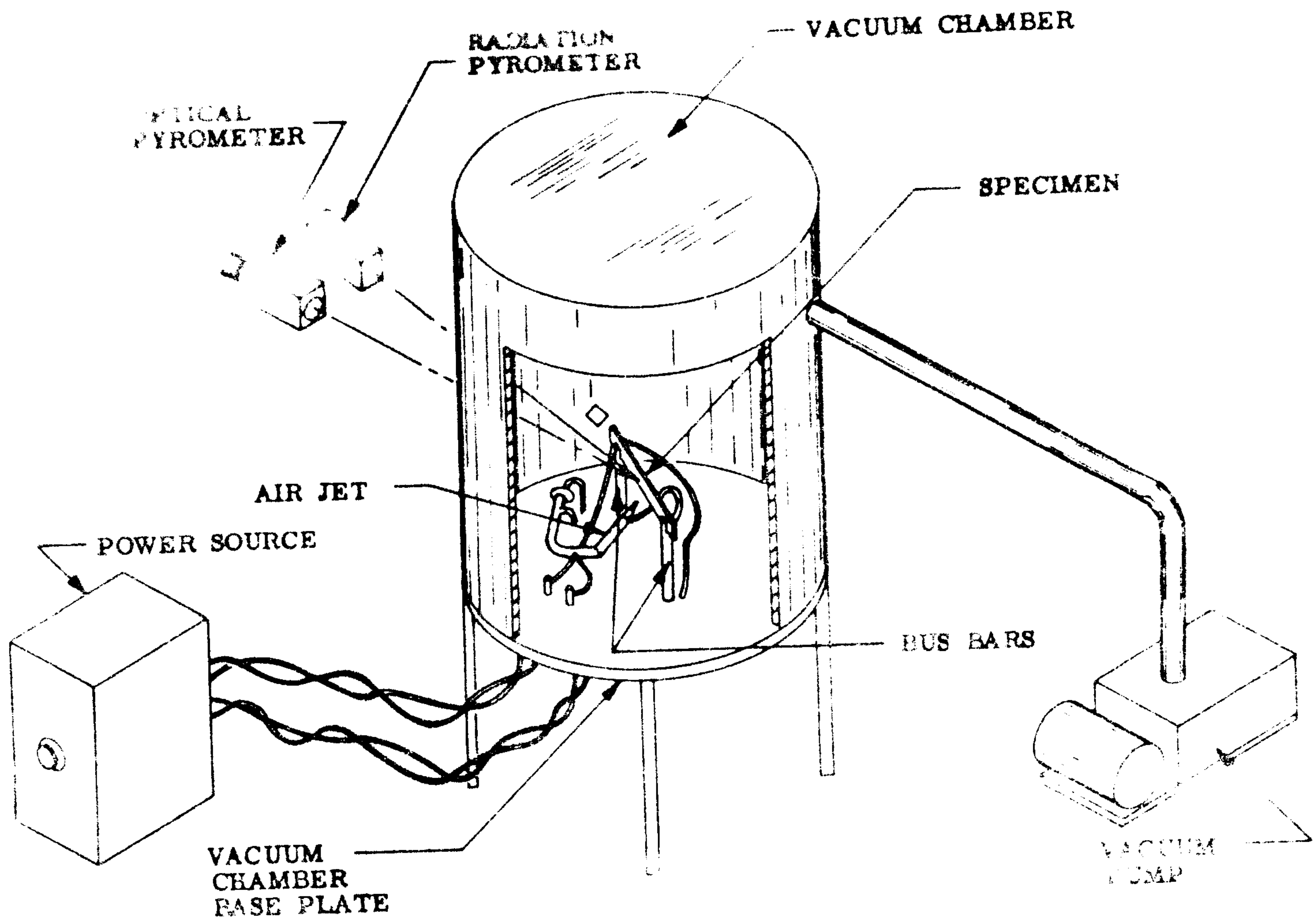

ENVIRONMENTAL SIMULATOR

FIG. 7